

# Batch-micromachined RPAs for Plasma and Ion Measurements

**Authors:** E. V. Heubel, A. I. Akinwande, L. F. Velásquez-García

**Sponsorship:** NASA

Retarding potential analyzers (RPAs) were first developed in the 1960's. RPAs find widespread application including characterization of near-spacecraft environments and assessment of the propulsion efficiency of plasma-based space thrusters. In this project we are exploring the multiplexing and scaling-down limits of RPAs using micro and nanotechnology. Miniaturized RPAs will weigh visibly less, which will reduce the cost of a nanosatellite-based mission. Also, miniaturized RPAs will provide better diagnostics of spacecraft plasma plumes as smaller projected area will be less disruptive to plasma under observation. In addition, batch-fabricated miniaturized RPAs can be used as part of a spacecraft "sensorial skin" that provides detailed local information of the plasma surrounding the spacecraft, particularly during re-entry, when monitoring exterior conditions is essential to ensuring safety during the mission.

An improvement of our work from the state-of-the-art RPAs is the introduction of *enforced aperture alignment*. When the apertures of each successive grid are aligned, the optical transparency of the sensor increases, which should result in improved signal strength. We recently developed a first-generation prototype of a hybrid microRPA (Figure 1). The hybrid microRPA has micromachined electrodes and a stainless steel housing. Internal dynamics of this type of energy analyzer, however, are more complex than simple transmission or reflection of the various ion species [1][2]. This fact is made evident by the experimental characterization of the microRPA using a commercial thermionic ion source for mass spectrometry. Figure 2 shows that the measured data reveal a peak in the energy distribution function around 5.4 V of retarding potential when the ionization region is at 10 V. Therefore, the observed ion energy distribution (dotted) deviates from the expected (continuous line) by approximately 4.6 V, a shift that is constant for a wide range of ionization region potentials. We speculate that changes in the internal dynamics due to enforced aperture alignment, sources of error in the applied voltages due to the materials selected, or a combination thereof are cause for this anomaly. Exploration of these potential sources of error continues, as well as the manufacturing of a fully batch-microfabricated RPA sensor with housing based on 3D HV packaging technology [3][4].

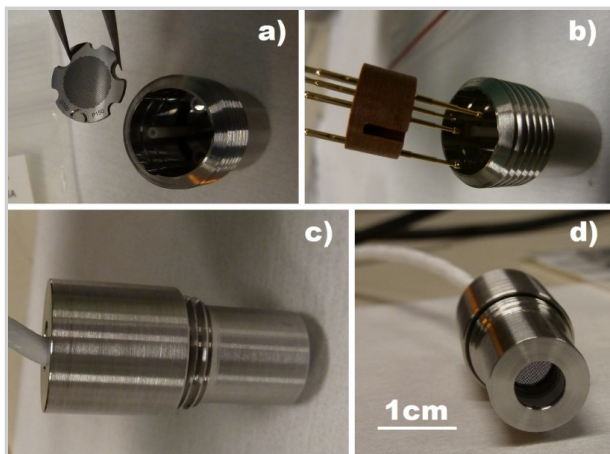


Figure 1: Assembly of a hybrid RPA. a) Micromachined grids are placed in a stainless steel housing, alumina spacers and guiderails enforce alignment and separation distance. b) Contact is made to each tungsten-coated electrode through gold pogo pins. c) and d) Completed assembly.

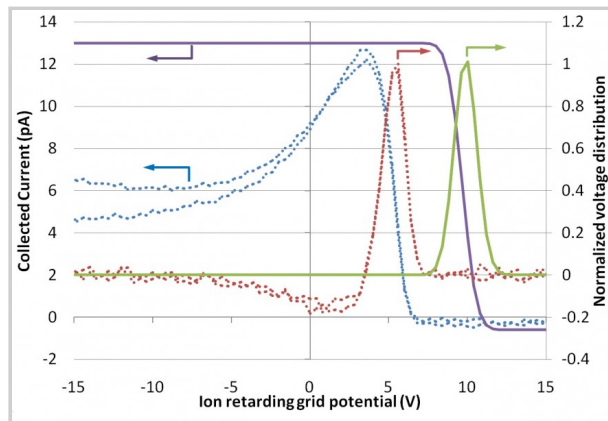


Figure 2: Experimental RPA data. Ions generated with a thermionic source at -50 eV energy and 0.2 mA emission current are accelerated through 10 V of potential. The figure shows the measured (dotted) and expected (continuous line) data.

1. C. K. Chao and S.-Y. Su, "Charged particle motion inside the retarding potential analyzer," *Physics of Plasmas*, vol. 7, no. 1, pp. 101-107, Jan. 2000. [↔]
2. C. L. Enloe and J. R. Shell, 2<sup>nd</sup>, "Optimizing the energy resolution of planar retarding potential analyzers," *Review of Scientific Instruments*, vol. 63, no. 2, pp. 1788-1791, Feb. 1992. [↔]
3. L. F. Velásquez-García, A. I. Akinwande, and M. Martínez-Sánchez, "Precision hand assembly of MEMS subsystems using DRIE-patterned deflection spring structures: An example of an out-of-plane substrate assembly," *Journal of Microelectromechanical Systems*, vol. 16, no. 3, pp. 598-612, 2007. [↔]
4. B. Gassend, L. F. Velásquez-García, and A. I. Akinwande, "Precision in-plane hand assembly of bulk-microfabricated components for high-voltage MEMS arrays applications," *Journal of Microelectromechanical Systems*, vol. 18, no. 2, pp. 332-346, Apr. 2009. [↔]

# Electron-impact-ionization Pump Using Double-gated Isolated Vertically Aligned Carbon Nanotube Arrays

Authors: V. Jayanty, X. Wang, A. I. Akinwande, L. F. Velásquez-García

Sponsorship: DARPA

There is a need for microscale vacuum pumps that can be readily integrated with other MEMS and electronic components at the chip-scale level. Vacuum pumps exhibit favorable scaling and are promising for a variety of applications such as portable mass spectrometers<sup>[1]</sup> and vacuum amplifiers. This project aims to develop the technology for a micro-fabricated electron-impact-ionizer pump. The micropump consists of a field-emission electron source that is an array of double-gated isolated vertically aligned carbon nanotubes (VA-CNTs), an electron-impact-ionization region, and an ion implantation getter, as shown in Figure 1. The pump works as follows: first, electrons are field-emitted from the VA-CNT array; then, the electrons are accelerated at a bias voltage that maximizes the probability of collision with neutral gas molecules, this way achieving ionization by fragmentation of the molecules; finally, ions are implanted into the getter.

In a double-gated field-emitter array, the first gate (extractor) is used to modulate the tunneling of electrons out of the tip, while the second gate (focus) is biased at a lower voltage than the first gate to focus the emitted electrons and to collect the back-streaming ions, thus protecting the tip<sup>[2]</sup>. As part of this work, we designed and fabricated single-gated isolated VA-CNT field-emission arrays, shown in Figure 2(a), to quantify the effectiveness of the field emitter-extractor diode to enhance the electric field on the emitter tip (i.e., estimate the extractor field factor), through experiments and simulations using the commercial software COMSOL. Figure 2(b) shows the solution of electric field using the same geometry of the device we fabricated. Each emitter has a 15-nm tip radius and 2- $\mu\text{m}$  height with a 1- $\mu\text{m}$  aperture from a single gate. From the simulation results we obtain an extractor field factor of  $7.35 \times 10^5 \text{V/cm}$ . Figure 2(c) is the experimental FN plot of an array of  $\sim 10,000$  single-gated emitters. From the slope of the plot we estimate a field factor of  $7.8 \times 10^5 \text{V/cm}$ , which is in good agreement with the prediction of the extractor field factor from the COMSOL simulation.

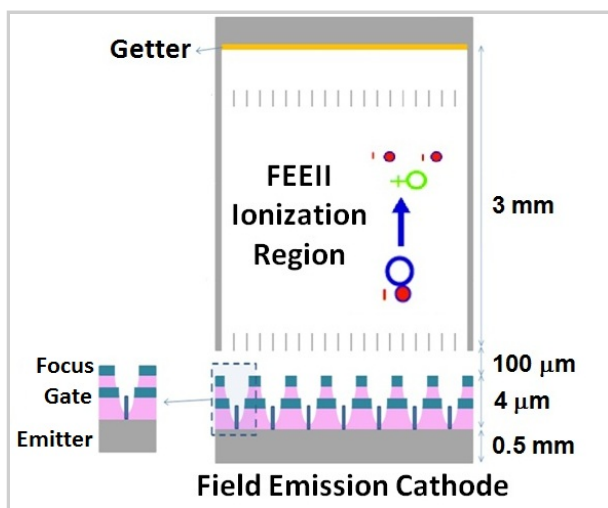


Figure 1: Electron-impact-ionization pump structure consists of a field-emission cathode (CNTs, an extractor gate and a focus gate), an electron-impact-ionization region (length of  $L=3\text{mm}$ ) and an ion-implantation getter.

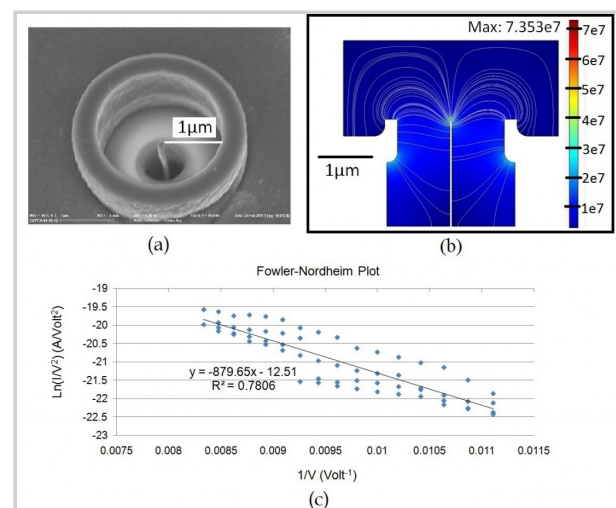


Figure 2: (a) SEM of single-gated isolated VA-CNT. (b) The solution of the electric field for an emitter with 15-nm tip radius, 2- $\mu\text{m}$  height, and 1- $\mu\text{m}$  gate aperture. A field factor ( $\beta_G$ ) of  $7.35 \times 10^5 \text{V/cm}$  is obtained. (c) The Fowler-Nordheim plot for an array of  $\sim 10,000$  emitters. A field factor ( $\beta_G$ ) of  $7.8 \times 10^5 \text{V/cm}$  is calculated.

1. K. H. Gilchrist, C. A. Bower, M. R. Lueck, J. R. Piascik, B. R. Stoner, S. Natarajan, C. B. Parker, and J. T. Glass, "A novel ion source and detector for a miniature mass spectrometer," *IEEE Sensors*, pp. 1372-1375, Oct. 2007. [↗]
2. L.-Y. Chen, L. F. Velásquez-García, X. Wang, K. Cheung, K. Teo, and A.-I. Akinwande, "Design, fabrication and characterization of double-gated vertically aligned carbon nanofiber field emitter arrays," in *Vacuum Nanoelectronics Conference*, 2007, pp. 82-83. [↗]

# Electrospray Nanodeposition of Liquids on Electrospun Nanofiber Mats for Low-cost Biochemical Sensing

**Authors:** E. V. Heubel, M. Overlin, K. Senecal (US Army NSRDEC), P. Marek (US Army NSRDEC), L. F.

Velásquez-García

**Sponsorship:** US Army

An electrospray emitter ionizes polar liquids using high electrostatic fields. The electric field produces suction on the free surface (meniscus) of an electrically conductive liquid, and the surface tension of the liquid tends to counteract the effect of the electrostatic suction. If the electric field is larger than a certain threshold, the meniscus snaps into a conic shape called a Taylor cone<sup>[1]</sup> (Figure 1). A Taylor cone emits charged particles from its apex due to the high electrostatic fields present there; these particles can be ions, droplets, fibers, etc., depending on the working liquid and the emitter flowrate<sup>[2]</sup>. In particular, electrospray in cone-jet mode<sup>[3]</sup> creates near-monodispersed charged droplets that can be used for many applications including mass spectrometry<sup>[4]</sup>, etching<sup>[5]</sup>, and nanosatellite propulsion<sup>[6]</sup>. In this project we are exploring electrospray in cone-jet mode as a technology to create controlled coating of electrospun nanofiber mats (Figure 2) with liquids such as fluorescent dye and nanoparticles solutions, as an alternative technology to nano-pipetting or ink jet printing. The long-term goal of the project is to investigate the design space of the technology to make low-cost and low false-positive biochemical detectors through the exploration of the multiplexing and scaling-down limits of cone-jet mode electrospray sources using batch micro- and nanofabrication<sup>[7]</sup>.

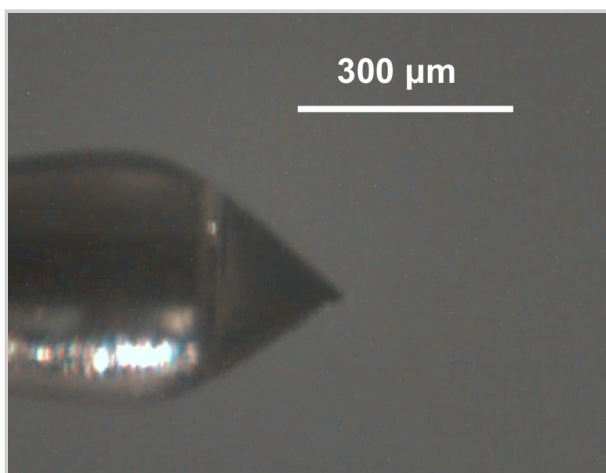


Figure 1: A Taylor cone at the end of a 300-µm OD capillary. Charged droplets are emitted from the apex of the cone. The working liquid is fluorescent dye.

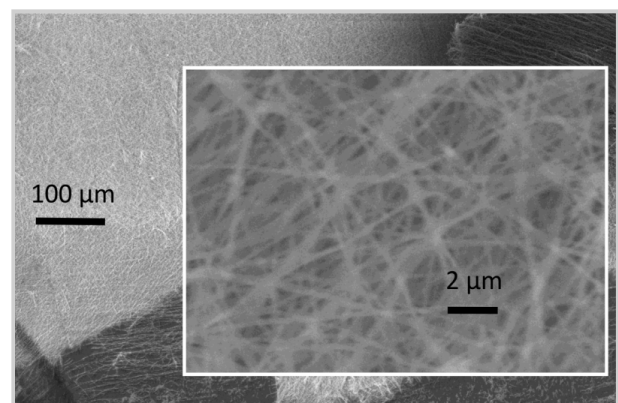


Figure 2: An unwoven mat of electrospun nanofibers. Using a solvent-polymer mix, electrospray emitters can generate conformal nanofiber mats with very high surface-to-volume ratio.

1. G. I. Taylor, "Disintegration of water drops in an electric field," *Proc. R. Soc. London A* vol. 280, pp. 383 – 397, 1964. [↔]
2. J. Fernandez de la Mora, "The fluid dynamics of Taylor cones," *Ann. Rev. of Fluid Mech.*, vol. 39: pp. 217– 243, 2007. [↔]
3. J. Fernandez de la Mora, "The current emitted by highly conductive Taylor cones," *J. Fluid Mech.*, vol. 260, pp. 155 – 184, 1994. [↔]
4. J. B. Fenn, M. Mann, C. K. Meng, S. F. Wong, and C. M. Whitehouse, "Electrospray ionization for mass spectrometry of large biomolecules," *Science*, vol. 246, no. 4926, pp. 64-71, 1989. [↔]
5. M. Gamero-Castaño and M. Mahadevan, "Sputtering of silicon by a beamlet of electrosprayed nanodroplets," *Appl. Surf. Sci.*, vol. 255, pp. 8556-8561, 2009. [↔]
6. L. F. Velásquez-García, A. I. Akinwande, and M. Martinez-Sanchez, "A planar array of micro-fabricated electrospray emitters for thruster applications," *J. of Microelectromech. Syst.*, vol. 15, no. 5, pp. 1272–1280, 2006. [↔]
7. B. Gassend, L. F. Velásquez-García, A. I. Akinwande, and M. Martinez-Sanchez, "A microfabricated planar electrospray array ionic liquid ion source with integrated extractor," *J. of Microelectromech. Syst.*, vol. 18, no. 3, pp. 679 – 694, 2009. [↔]

# MEMS Langmuir Probes for Atmospheric Reentry Plasma Diagnostics

**Authors:** E. S. Field, A. I. Akinwande, L. F. Velásquez-García

**Sponsorship:** NASA

One of the most fundamental technical problems concerning spacecraft design is preparing the vehicle to survive the extreme conditions encountered during reentry into the Earth's atmosphere<sup>[1]</sup>. When a hypersonic vehicle travels through the atmosphere, a high-density, low-temperature plasma sheath forms around it<sup>[2]</sup>. The reentry plasma sheath affects heat transfer to the spacecraft, aerodynamics, and perhaps most notably, communications. A communications blackout is a major threat, bringing about a complete loss of RF signal strength between the reentry vehicle and the ground. A thorough knowledge of reentry plasma sheath properties is needed to effectively develop systems capable of maintaining communications during reentry. However, the reentry plasma sheath occurs due to processes that are not well understood. Furthermore, the conditions of the plasma sheath rapidly change throughout reentry, which introduces additional complications. Analytical approaches alone are not sufficient to gain a complete understanding of the plasma sheath. Therefore, instrumentation must be developed to measure properties of the plasma sheath during reentry<sup>[3]</sup>.

We propose a novel approach to reentry plasma diagnostics, utilizing planar arrays of MEMS Langmuir probes to perform real-time measurements of the electron temperature and number density of the reentry plasma sheath. The MEMS Langmuir probes, shown in Figure 1, consist of an array metallic vias in a high temperature-resistant dielectric substrate, which can be blended onto the outer surface of a reentry vehicle (i.e., as a sensorial skin). Figure 2 shows one of the early prototypes we made as proof of concept of the device process flow. The MEMS Langmuir probes are made using electroplated gold and an ultrasonic drilled Pyrex substrate. The performance of the MEMS probes will be validated experimentally in laboratory plasmas similar to those encountered by spacecraft during reentry.

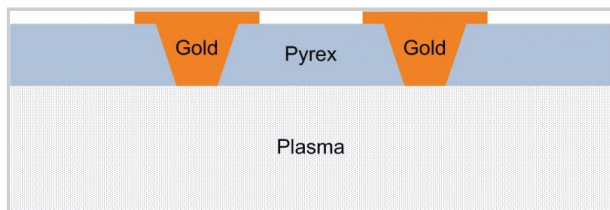


Figure 1: Cross section schematic of the arrays of MEMS Langmuir Probes. The tapered vias facilitate metal filling-in.

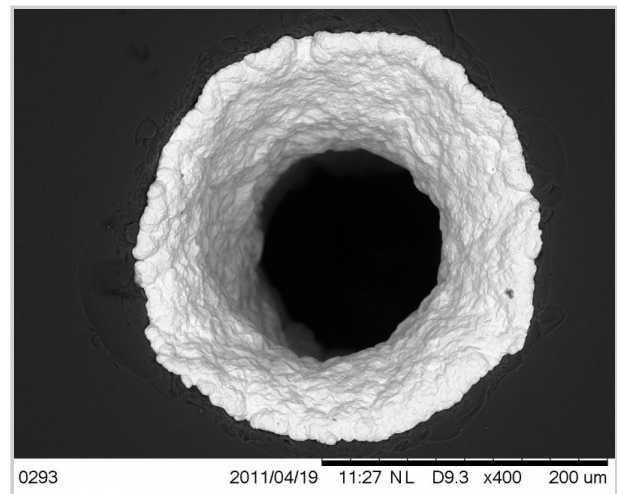


Figure 2: SEM of a MEMS Langmuir probe test structure as seen from the plasma. Gold was electroplated into vias that were machined into a Pyrex substrate. In the test structure, the vias were partially filled to characterize film conformality and processing parameters. Longer electroplating time will result in completely filled-in vias, hence forming arrays of MEMS Langmuir probes.

1. L. C. Scalabrin and I. D. Boyd, "Numerical simulation of weakly ionized hypersonic flow for reentry configurations," in *9<sup>th</sup> AIAA/ASME Joint Thermodynamics and Heat Transfer Conf.*, 2006 © AIAA. DOI: 2006-3773. [↗]
2. K. M. Lemmer, A. D. Gallimore, and T. B. Smith, "Using a helicon source to simulate atmospheric re-entry plasma densities and temperatures in a laboratory setting," *IEEE Plasma Sources Sci. Technol.*, vol. 18, no. 2, May 2009. [↗]
3. J. P. Rybak and R. J. Hill, "Progress in reentry communications," *IEEE Transactions on Aerospace and Electronic Systems*, vol. aes-7, no. 5, pp. 879-894, Sept. 1971. [↗]

# Scaling of High Aspect Ratio Current Limiters for the Individual Ballasting of Large Arrays of Field Emitters

Authors: S. A. Guerrero, L. F. Velasquez-Garcia, A. I. Akinwande

Sponsorship: DARPA

Field Emitter Arrays (FEAs) are excellent cold cathodes, but they have not found widespread adoption in demanding device applications because of several major challenges, including spatial/temporal current variations emanating from emitter tip radius distribution and the work function fluctuation. A consequence of tip radius variation is that the sharper emitters burn out from Joule heating before duller emitters turn on, reducing the current attainable from FEAs.

Addressing these challenges, groups have incorporated current limiting (ballasting) elements including large resistors<sup>[1]</sup>, diodes<sup>[2]</sup>, and MOSFETs<sup>[3]</sup> into FEAs, but none of these simultaneously provide high current, high emitter density, and high current density. Velasquez-Garcia et al. demonstrated silicon vertical ungated FETs integrated with FEAs, resulting in a Si tip on Si pillar structure<sup>[4]</sup>. The ungated FET has a current-source-like I-V characteristic, providing effective individual ballasting of emitters while allowing uniform and high current emission without thermal runaway<sup>[4]</sup>. To limit emission current, the device uses pinch-off and velocity saturation of carriers in a Si high aspect ratio channel. Their pillars have a diameter of 1  $\mu\text{m}$ , height of 100  $\mu\text{m}$ , and 10- $\mu\text{m}$  pitch, resulting in a density of  $10^6$  emitters/ $\text{cm}^2$ . However, a consequence of tip radius variation and ballasting is that the energy distribution of emitted electrons is larger when compared to un-ballasted FEAs.

To obtain FEAs with higher current densities, lower operating voltages, and reduced energy spread while retaining current uniformity, we expanded on previous work by scaling their tip on Si pillar structure. We developed vertical ungated FET current limiters 100 nm in diameter, 8  $\mu\text{m}$  tall, and with 1- $\mu\text{m}$  pitch, increasing the density to  $10^8$  emitters/ $\text{cm}^2$  (Figure 1). These devices demonstrate excellent current saturation of 15 pA / pillar with a linear conductance of  $2.6 \times 10^{-10}$  S/pillar and an output conductance under  $10^{-13}$  S/pillar. The current saturates at a drain to source voltage under 0.2 V. These are the highest density, smallest diameter, and lowest operating voltage Si vertical ungated FETs ever reported.

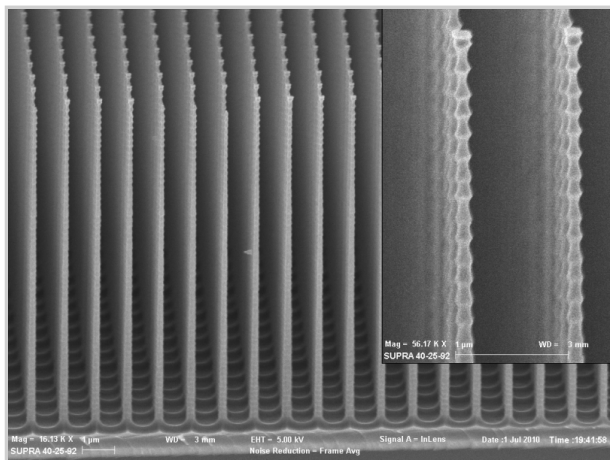


Figure 1: Cross-sectional SEM of the vertical ungated FET structure with the passivation oxide removed. The pillars are 8 microns tall and taper to a diameter of 95 nm at the top.

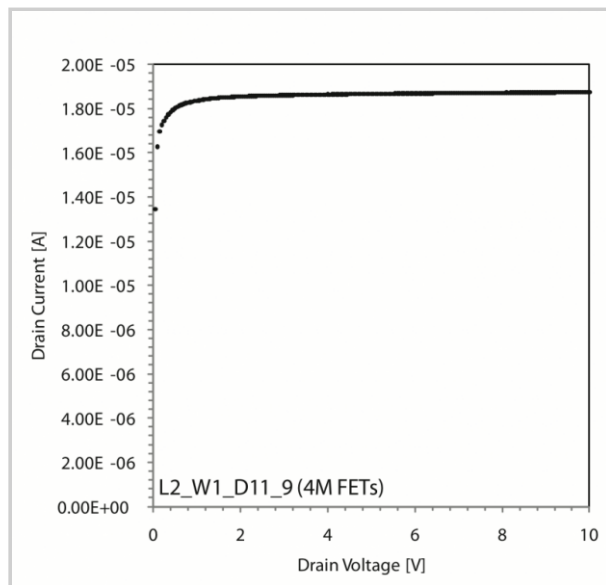


Figure 2: Output characteristics of large arrays show good saturation at low  $V_{ds}$ .

1. P. Vaudaine and R. Meyer, "Microtips' fluorescent display," *IEDM Tech. Dig.*, 1991, pp. 197-200. [[↔](#)]

2. Y. Kobori and M. Tanaka, "Field emission cathode," U.S. Patent 5 162 704, Feb. 5, 1992. [[↔](#)]

3. J. Itoh, T. Hirano, and S. Kanemaru, "Ultrastable emission from a metal-oxide-semiconductor field-effect transistor-structured Si emitter tip," *Applied Physics Letters*, vol. 69, no. 11, pp. 1577-1578, 1996. [[↔](#)]

4. L. F. Velasquez-Garcia, S. A. Guerrero, Y. Niu, and A. I. Akinwande, "Uniform high-current cathodes using massive arrays of Si field emitters individually controlled by vertical Si ungated FETs – Part 1: Device design and simulation & Part 2: Device fabrication and characterization." *IEEE Trans. Electron Devices*, vol. 58, no. 6, pp. 1775-1791, June 2011. [[↔](#)] [[↔](#)]

# Luis Fernando Velásquez-García

Principal Research Scientist

Microsystems Technology Laboratories

## *Collaborators*

---

A.I. Akinwande, EECS, MIT

V. Hruby, Busek Co.

C. Livermore, MechE, MIT

P. Marek, US Army NSRDEC

M.A. Schmidt, EECS, MIT

K. Senecal, US Army NSRDEC

S. Taylor, University of Liverpool

## *Postdoctoral Associates*

---

K. Cheung (co-supervised with A.I. Akinwande)

X. Wang (co-supervised with A.I. Akinwande)

## *Graduate Students*

---

E. Field, Research Assistant, MechE

E. V. Heubel, Research Assistant, MechE (co-supervised with A.I. Akinwande)

S. Guerrero, Research Assistant, EECS (co-supervised with A.I. Akinwande)

V. Jayanti, Research Assistant, EECS

D. Jeng, Research Assistant, EECS (co-supervised with A.I. Akinwande)

## *Undergraduate Students*

---

M. R. Overlin

## *Support Staff*

---

C. Collins, Admin. Asst. II

## *Publications*

---

F. Eid, L. F. Velásquez-García, and C. Livermore, “Design, Fabrication, and Demonstration of a MEMS Steam Generator for Ejector Pump Applications”, *Journal of Micromechanics and Microengineering*, Vol. 20, No. 20, 104007, 2010.

K. Cheng, L. F. Velásquez-García, and A. I. Akinwande, “Chip-Scale Quadrupole Mass Filters for Portable Mass Spectrometry”, *Journal of Microelectromechanical Systems*, Vol. 19 No. 3, pp. 469–483, 2010.

L. F. Velásquez-García, B. Gassend, and A. I. Akinwande, “CNT-based MEMS Ionizers for Portable Mass Spectrometry Applications”, *Journal of Microelectromechanical Systems*, Vol. 19, No. 3, pp. 484–493, 2010.

B. Gassend, L. F. Velásquez-García, and A. I. Akinwande, “Design and Fabrication of DRIE-Patterned Complex Needle-Like Structures”, *Journal of Microelectromechanical Systems*, Vol. 19, No. 3, pp. 589–598, 2010.

T. J. Hogan, S. Taylor, K. Cheung, L. F. Velásquez-García, A. I. Akinwande, and R. E. Pedder, “Performance Characteristics of a MEMS Quadrupole Mass Filter with Square Electrodes – Experimental and Simulated Results”, *IEEE Transactions on Instrumentation and Measurement*, Vol. 59, No. 9, pp. 2458 – 2464, 2010.

K. Cheung, L. F. Velásquez-García, and A. I. Akinwande, “High-Performance Square Electrode Quadrupole Mass Filters”, *Technical Digest 23<sup>rd</sup> IEEE International Conference on Micro Electro Mechanical Systems MEMS 2010*, Hong Kong, SAR, China, pp. 867 – 870, Jan. 24 – 28 2010.

F. Eid, L. F. Velásquez-García, and C. Livermore, “Design, Fabrication, and Demonstration of a MEMS Steam Generator for Ejector Pump Applications”, *Technical Digest 9<sup>th</sup> International Workshop on Micro and Nanotechnology for Power Generation and Energy Conversion Applications*, Washington DC, USA, pp. 41 – 44, December 1-4, 2009. (Article won best student oral presentation award).

L. F. Velásquez-García, B. Gassend, and A. I. Akinwande, “CNT-Based Gas Ionizers with Integrated MEMS Gate for Portable Mass Spectrometry Applications”, *Technical Digest of 15<sup>th</sup> International Conference on Solid-State Sensors, Actuators and Microsystems*, Denver CO, USA, pp. 1646-1649, June 21 – 25, 2009.

B. Gassend, L. F. Velásquez-García, A. I. Akinwande and M. Martinez-Sanchez, “A Microfabricated Planar Electrospray Array Ionic Liquid Ion Source with Integrated Extractor”, *Journal of Microelectromechanical Systems*, Vol. 18, No. 3, pp. 679 – 694, 2009.

B. Gassend, L. F. Velásquez-García, and A. I. Akinwande, “Precision In-Plane Hand Assembly of Bulk-Microfabricated Components for High Voltage MEMS Arrays Applications”, *Journal of Microelectromechanical Systems*, Vol. 18, No. 2, pp. 332 – 326, 2009.

L. F. Velásquez-García, K. Cheung, and A. I. Akinwande, “An Application of 3D MEMS Packaging: Out-Of-Plane Quadrupole Mass Filters”, *Journal of Microelectromechanical Systems*, Vol. 16, No. 6, pp. 1430–1438, 2008.

L. F. Velásquez-García and A. I. Akinwande, “Fabrication of Large Arrays of High-Aspect-Ratio, Single Crystal Silicon Columns with Isolated vertically Aligned Multi-Walled Carbon Nanotube Tips”, *Nanotechnology* 19, (2008) 405305. (Article was the cover page and featured article of the issue 40 of the IOP Journal Nanotechnology).